Atherosclerosis 288 (2019) 76–84

Contents lists available at ScienceDirect

Atherosclerosis

journal homepage: www.elsevier.com/locate/atherosclerosis

Suv39h1 downregulation inhibits neointimal hyperplasia after vascular injury

Jing Zhang[a,b], Jing Chen[c], Jun Yang[b], Changwu Xu[c], Qi Hu[c], Hui Wu[b], Wanyin Cai[a], Qing Guo[d], Wenqi Gao[a], Chao He[b], Chaojun Yang[a], Jian Yang[b,*]

[a] Central Laboratory, The First College of Clinical Medical Science, China Three Gorges University & Yichang Central People's Hospital, Yichang, 443003, China
[b] Department of Cardiology, The First College of Clinical Medical Science, China Three Gorges University & Yichang Central People's Hospital, Yichang, 443003, China
[c] Department of Cardiology, Renmin Hospital of Wuhan University, Wuhan, 430060, China
[d] Department of Ophthalmology, The First College of Clinical Medical Science, China Three Gorges University & Yichang Central People's Hospital, Yichang, 443003, China

HIGHLIGHTS

- Suv39h1 downregulation inhibits Ang II-stimulated migration and proliferation of VSMCs.
- Suv39h1 downregulation attenuates neointimal hyperplasia after vascular injury.
- Suv39h1 downregulation decreases Id3 production, and promotes p21 and p27Kip1 expression.

ARTICLE INFO

Keywords:
Suv39h1
Neointimal hyperplasia
Id3
p21
p27Kip1

ABSTRACT

Background and aims: Neointimal hyperplasia resulting from pathological vascular smooth muscle cells (VSMCs) activation is a common pathophysiological basis for numerous proliferative vascular diseases, such as restenosis. Suv39h1, an important transcription suppressor, may be involved in this process. Herein, we investigated the role of Suv39h1 in pathological intimal hyperplasia and its possible mechanisms *in vitro* and *in vivo*.
Methods: An adenovirus vector for Suv39h1 overexpression and a lentiviral vector for its downregulation were constructed and used to transfect cultured VSMCs *in vitro*. The functional changes in VSMCs stimulated by angiotensin II (Ang II) were observed and the possible mechanism was investigated. Additionally, rat carotid arteries with balloon injury were locally transfected with these viral vectors and changes in neointima formation, proliferating cell nuclear antigen (Pcna) expression and collagen deposition were examined.
Results: Upon Ang II stimulation, the expression of Suv39h1 and inhibitor of DNA binding 3 (Id3) was significantly increased. Suv39h1 downregulation inhibited Ang II-stimulated migration and proliferation of VSMCs, antagonized the production of Id3 and promoted p21 and p27Kip1 expression. In contrast, Suv39h1 overexpression had the opposite effects. Suv39h1 regulated the transcription of *p21* and *p27Kip1* by controlling H3K9me3 in the proximal promoter regions. Consistent with the VSMCs results, *Suv39h1* and *Id3* expression was significantly increased in blood vessels after balloon injury. Suv39h1 downregulation inhibited intimal hyperplasia, and attenuated Pcna expression and collagen synthesis in the intima, while Suv39h1 overexpression had the opposite effects.
Conclusions: Suv39h1 downregulation effectively inhibited neointimal hyperplasia after vascular injury.

1. Introduction

Although the incidence of in-stent restenosis significantly decreased by drug-eluting stents compared with bare metal stents, a few large clinical studies have shown that restenosis rates of first- and second-generation drug-eluting stents are still up to 14.6% and 12.2%, respectively. In particular, there were more incidences of multiple high-risk factors and complex vascular lesions, which are the leading causes of late stent complications [1].

The pathology of restenosis involves multiple steps. After injury of

* Corresponding author. Department of Cardiology, The First College of Clinical Medical Science, China Three Gorges University & Yichang Central People's Hospital, Yiling Road, Yichang, 443003, China.
E-mail address: yangjian@ctgu.edu.cn (J. Yang).

https://doi.org/10.1016/j.atherosclerosis.2019.06.909
Received 24 October 2018; Received in revised form 9 May 2019; Accepted 19 June 2019
Available online 20 June 2019

the vascular endothelium, the subendothelial matrix is exposed to peripheral circulating cells and various cytokines. Next, vascular smooth muscle cells (VSMCs) in the tunica media transform from contractile quiescent cells to synthetic cells. These proliferative and migratory VSMCs under the intima synthesize a number of extracellular matrix components and form the neointima. This results in loss of lumen area and decreased perfusion [2]. Increased VMSC proliferation, which is the basis of neointima formation, is a complex process and various protein-protein interactions are involved in ensuring this accurate biological process [3]. Cyclins and cyclin-dependent kinases (CDKs) play a positive role in regulating cell cycle progression, while CDK inhibitors (CDKIs) such as p21 and p27Kip1 are negative regulators of the cell cycle [4]. Increasing p21 or p27Kip1 expression suppresses VSMC proliferation and neointimal hyperplasia [5,6]. Inhibitor of DNA binding 3 (Id3), an important helix-loop-helix protein, forms a homodimer or heterodimer complex by binding with another type of helix-loop-helix (basic-helix-loop-helix, bHLH), to inhibit its DNA-binding activity, thus promoting cell growth and tumor formation [7]. A previous study suggests that Id3 expression *in vivo* is significantly increased on days 3 and 7 after vascular injury [8]. Additionally, upregulation of Id3 enhances VSMC growth and neointima formation in response to carotid injury [9]. Importantly, there is a certain interaction between Id3 and CDKIs including p21 and p27Kip1 [10,11], which provides new targets for the prevention of restenosis.

Suppressor of variegation 3–9 homolog 1 (Suv39h1), an important histone methylation enzyme, trimethylates histone H3 on lysine 9 (H3K9me3), results in transcriptional repression or silencing of target genes. However, some studies have shown that Suv39h1 plays complex regulatory roles as a transcription suppressor, including inhibition of proinflammatory genes and driving transcription of certain tumor-associated genes such as bcl-2 and c-myc [12]. Inhibition of Suv39h1 can increase p21 expression via suppression of histone H3K9me3 levels at the promoter of the *p21* gene [13], suggesting Suv39h1 is a potential therapeutic target against VSMC proliferation. Nevertheless, Suv39h1 has been poorly investigated in cardiovascular diseases, especially restenosis. Additionally, whether *p27Kip1* or *Id3* can be regulated by H3K9me3 modification via alteration of Suv39h1 expression is still unclear. Therefore, we examined whether Suv39h1 can regulate neointimal hyperplasia after vascular injury completely or partially via H3K9me3 modification at the promoter of *Id3/p27/p27Kip1*.

Herein, we constructed an adenovirus vector for Suv39h1 overexpression (Ad-Suv39h1) and a lentiviral vector for Suv39h1 downregulation (LV-Suv39h1), and used them to transfect VSMCs cultured *in vitro*. We observed the functional changes in the cells under angiotensin II (Ang II) stimulation and attempted to elucidate the mechanisms of these effects. In addition, rat carotid arteries after balloon injury were locally transfected with the virus vectors described above and the effects on neointima formation was examined. The long-term goal of this research was to identify new clinical intervention targets for proliferative vascular diseases such as restenosis.

2. Materials and methods

2.1. Culture and virus transfection of rat vascular smooth muscle cells

All animal experimental protocols were approved by the Institutional Animal Care and Use Committee of China Three Gorges University and conformed to the Guide for the Care and Use of Laboratory Animals by the National Institutes of Health. Male Sprague Dawley (SD) rats (120–150 g, SPF grade, provided by the Experimental Animal Center of China Three Gorges University) were anesthetized with 2% pentobarbital sodium (Sigma) at a dose of 40 mg/kg. After bluntly separating the thoracic aorta along the spine, we cut both ends with ophthalmic scissors and placed the aortic segment in fresh Dulbecco's modified Eagle's medium (Hyclone). Connective tissue and adventitia surrounding the arteries were removed together with the endothelium. The blood vessels were washed and cut into 2 × 2 mm tissue pieces and placed in a petri dish with an endothelial surface. After incubation for 20 min at 37 °C in a 5% CO_2 atmosphere, medium with 20% serum (Hyclone) was added. The medium was replaced at 3-d intervals. When confluence of the attached cells reached 80%–90%, they were subcultured at a ratio of 1:2 or 1:3. Cells were used for experiments at passages 3–5.

VSMCs in logarithmic growth were transfected with Ad-Suv39h1 or a control vector (Ad-Null) at multiplicity of infection (MOI) = 15 for 4 h. They were then cultured in medium with 10% fetal bovine serum (FBS) for 3 d. VSMCs in logarithmic growth were transfected with LV-Suv39h1 or the control vector (LV-NC) at MOI = 40 for 12 h, in the presence of polybrene at a final concentration of 5 μg/ml. The cells were further cultured in medium with 10% FBS for 5 d. These stably transfected VSMCs were used for the various intervention experiments.

2.2. Viral vector construction

The adenoviral vector carrying the rat *Suv39h1* gene was constructed by Vector Gene Technology Company Limited (Beijing, China). Briefly, the *Suv39h1* cDNA was cloned into the adenovirus shuttle plasmid, pDC316, and co-transfected with adenoviral backbone plasmids into 293 cells to generate Suv39h1 adenoviruses (Ad-Suv39h1). After amplification, purification and PCR identification, an Ad-Suv39h1 vector stably overexpressing Suv39h1 with an infective titer of 5×10^9 pfu/mL was obtained. pDC316 with cloned green fluorescent protein (GFP) was used to generate the control adenovirus (Ad-Null).

Four siRNA sequences for *Suv39h1* were designed to synthesize shRNA-containing DNA sequences *in vitro* (Table 1). After double enzyme digestion, the linearized GV118 vector and the synthesized DNA fragments were ligated and transformed, and positive clones were selected for sequencing and identification (Genechem, Shanghai, China). After co-transfection of GV118-*Suv39h1* shRNA with lentiviral packaging plasmids into 293T cells, lentiviruses (LV-Suv39h1) were produced. The four different LV-Suv39h1 plasmids were then used to infect isolated VSMCs at MOI of 40, and the steady-state mRNA level of

Table 1
Suv39h1-specific shRNA oligonucleotide sequences at 5′, stem, loop, stem, and 3′ areas.

NO.	5′	STEM	Loop	STEM	3′
Suv39h1-RNAi(KD1)-a	T	GGACAACAGCTTGCCGAAA	CTCGAG	TTTCGGCAAGCTGTTGTCC	TTTTTTC
Suv39h1-RNAi(KD1)-b	TCGAGAAAAAA	GGACAACAGCTTGCCGAAA	CTCGAG	TTTCGGCAAGCTGTTGTCC	A
Suv39h1-RNAi(KD2)-a	T	CAGAAAGGCATCCGCTACA	CTCGAG	TGTAGCGGATGCCTTTCTG	TTTTTTC
Suv39h1-RNAi(KD2)-b	TCGAGAAAAAA	CAGAAAGGCATCCGCTACA	CTCGAG	TGTAGCGGATGCCTTTCTG	A
Suv39h1-RNAi(KD3)-a	T	CACTGCAGGTGTACAACGTAT	CTCGAG	ATACGTTGTACACCTGCAGTG	TTTTTTC
Suv39h1-RNAi(KD3)-b	TCGAGAAAAAA	CACTGCAGGTGTACAACGTAT	CTCGAG	ATACGTTGTACACCTGCAGTG	A
Suv39h1-RNAi(KD4)-a	T	AAGCTTTCTTGTCCTGCCCTT	CTCGAG	AAGGGCAGGACAAGAAAGCTT	TTTTTTC
Suv39h1-RNAi(KD4)-b	TCGAGAAAAAA	AAGCTTTCTTGTCCTGCCCTT	CTCGAG	AAGGGCAGGACAAGAAAGCTT	A

Suv39h1 was determined by qRT-PCR. The LV-Suv39h1 with the most robust knockdown effect was used for the following experiments. GV118 containing a control shRNA sequence that targets unknown rat genes was used to generate control lentiviruses (LV-NC). The final titers of these four recombinant lentivirus vectors were 7.5×10^8 TU/ml, 2×10^9 TU/ml, 2.5×10^9 TU/ml and 2×10^9 TU/ml.

2.3. Carotid balloon injury model and local viral transfection

Seventy-two male SD rats (350–400 g) were randomly divided into six groups (n = 12 in each group): sham operation, model, Ad-Null, Ad-Suv39h1, LV-NC and LV-Suv39h1. The rats were anesthetized, immobilized and sterilized. The skin covering the trachea was cut to separate and expose the left common carotid, internal carotid and external carotid arteries. Then, 50 U/ml heparin sodium was injected at a dose of 100 U/kg. A 1.25 F balloon with a guide wire (balloon diameter 1.25 mm, balloon length 1 mm, Medtronic) was inserted into the common carotid artery from the external carotid incision. After filling the balloon, it was moved back and forth three times in the blood vessel. After the pressure pump returned to zero, the balloon and guidewire were withdrawn. Following completion of the balloon injury, blood was washed from the surgical field of vision with normal saline. The proximal ends of the internal carotid and common carotid arteries were clamped with micro-artery clips to block blood flow in the balloon-injured segment. Because of the limited volume of the injured artery and the need for optimal transfection efficiency *in vivo*, virus stock solutions (5×10^9 pfu/ml in the Ad groups, 7.5×10^8 TU/ml in the LV groups and equal volumes of normal saline in the control groups) were administered with an insulin needle as previously described [14]. After 20 min of local transfection, the blood flow was restored in the common and internal carotid arteries. The wound was then sutured and disinfected layer by layer. Rats were euthanized by anesthesia to harvest arterial samples after 7 or 28 days of conventional maintenance in the animal facility.

2.4. Detection of cell migration by the transwell assay

Cells (10^5 cells in 200 μl) were planted in the upper chamber of a Transwell apparatus (Corning) and stimulated with 0.2 μg/ml Ang II (Peprotech) in the lower chamber for 8 h. Then, the upper chamber was removed and cells that had not migrated were gently wiped off with a swab. After washing and fixing with methanol, the Transwell membranes were stained with 0.1% crystal violet for 15 min, and then washed and allowed to dry at room temperature. Under the 100× objective of a microscope, cells in the upper, middle, lower, left and right visual fields were counted, and the sum of these counts represents the number of migrating cells in the chamber.

2.5. Western blot analysis

Western blot analysis was performed as previously described [14]. The total cellular protein of cell pellets was extracted with RIPA lysis buffer (Beyotime). After quantification by the BCA method (Beyotime), the samples were denatured. Proteins were separated by 12% SDS-PAGE (Beyotime) and transferred to PVDF membranes for western blotting. Membranes were incubated with primary antibodies for Suv39h1 (1:800; Abcam), Pcna (1:300; Bioss), Gapdh (1:1000; Cell Signaling), Id3 (1:800; Abcam), p21 (1:200; Abcam) and p27Kip1 (1:200; Abcam), followed by secondary antibodies (1:1500–1:2000; Boster) diluted in blocking solution. An electrochemiluminescence (ECL) kit (Beyotime) was used to visualize immunostained bands. Quantity one image analysis software was used to determine the optical densities of the bands, and the optical density of Gapdh was used as a standard to calculate the relative level of each protein.

2.6. Real-time PCR analysis

Seven days after surgery, homogenates of common carotid arterial samples from the injured side were prepared. Total RNA was extracted by the TRIzol method (Invitrogen), reverse transcribed into cDNA and stored at −80 °C. The cDNA was added to the reaction system and predenatured at 95 °C for 10 min, denatured at 95 °C for 10 s, and annealed and extended at 60 °C for 60 s. A total of 40 cycles of real-time PCR amplification was performed and data were collected. Statistical analysis was conducted using the $2^{-\Delta\Delta Ct}$ method. The following primer sequences were used:

Suv39h1: forward 5′-CGTGGATGCCGCCTATTATG-3′; reverse 5′-GGGGTAGTCGCTCATCAAGGT-3′ *Id3*: forward 5′-TGCCACAGCCCT CTTCATTT-3′; reverse 5′-CAGGCCACCCAAGTTCAGTC-3′ *p21*: forward 5′-AGTATGCCGTCGTCTGTTCG-3′; reverse 5′-GAGTGCAAGACAGCGA CAAG-3′ *p27Kip1*: forward 5′-GATACGAGTGGCAGGAGGTG -3′; reverse 5′-TCTGACGAGTCAGGCATTTG-3′ *Gapdh*: forward 5′-GGAAAGCTGTG GCGTGAT-3′; reverse 5′-AAGGTGGAAGAATGGGAGTT-3′.

2.7. Chromatin immunoprecipitation assay

Chromatin immunoprecipitation (ChIP) assays were performed with ChIP kits (Millipore) as previously described [14]. Briefly, VSMCs were grown to 60% confluence, and then infected with LV-NC or LV-Suv39h1 for 5 days. After stimulation with Ang II for 1 h, the cells were washed and crosslinked with 1% formaldehyde, which was stopped by 1.25 M glycine. The cell lysates were sonicated and subjected to immunoprecipitation with H3K9me3 antibody (Abcam) or IgG (Santa Cruz). Immune complexes were collected and eluted with buffer. Protein-DNA crosslinks were reversed, and the DNA was extracted. ChIP-enriched DNA samples were analyzed by real-time qPCR using primer sequences near the promoter site of *p21* and *p27kip1*. The data were analyzed using the $2^{-\Delta\Delta Ct}$ method and normalized against input samples. The results are expressed as fold change relative to the LV-NC group. The primer sequences used were:

Id3: forward 5′-CAGCTCTTCCTCATTCCGCG-3′; reverse 5′-GCTTCC TCTGGCTGGTCGG-3′ *p21*: forward 5′-AACCCTAAACATGGCATT CGC-3′; reverse 5′-GGCTCTAGCAGACCCTCAAAA-3′*p27Kip1*: forward 5′-AGGTTTCCTGGATCTTTCGCCTA-3′; reverse 5′-GCTAGTTCAACCCA CCTGCATTC-3′.

2.8. Histology

On day 28 after surgery the common carotid artery at the injured segment was harvested and fixed in 4% paraformaldehyde for 72 h. After 70%–100% ethanol gradient dehydration, xylene gradient vitrification and paraffin embedding, 4-μm sections were cut. Sections were dewaxed and hydrated, stained with hematoxylin-eosin (H&E) and photographed under a microscope. Image Pro Plus 6.0 image analysis software was used to measure the areas of the tunica media, neointima and blood vessel lumen, as well as to evaluate intimal hyperplasia in each injured vessel.

The vascular specimens were immersed in 3% H_2O_2 at room temperature for 10 min after vitrification, ethanol gradient dehydration and hydration. Microwave antigen retrieval and serum blocking were sequentially performed. Immunohistochemical staining with an antibody against Pcna (Bioss) and immunofluorescence staining with an antibody against H3K9me3 (Abcam) were performed. For the immunohistochemistry analysis, the number of positively stained cells was quantified from five random fields under 200× magnification. For the immunofluorescence staining, cell nuclei were stained with DAPI, and the fluorescence was observed under an immunofluorescence microscope. Masson trichrome staining was also performed on vessel sections and the collagen area ratio was calculated [collagen area ratio = collagen area/(collagen area + muscle area) × 100%)].

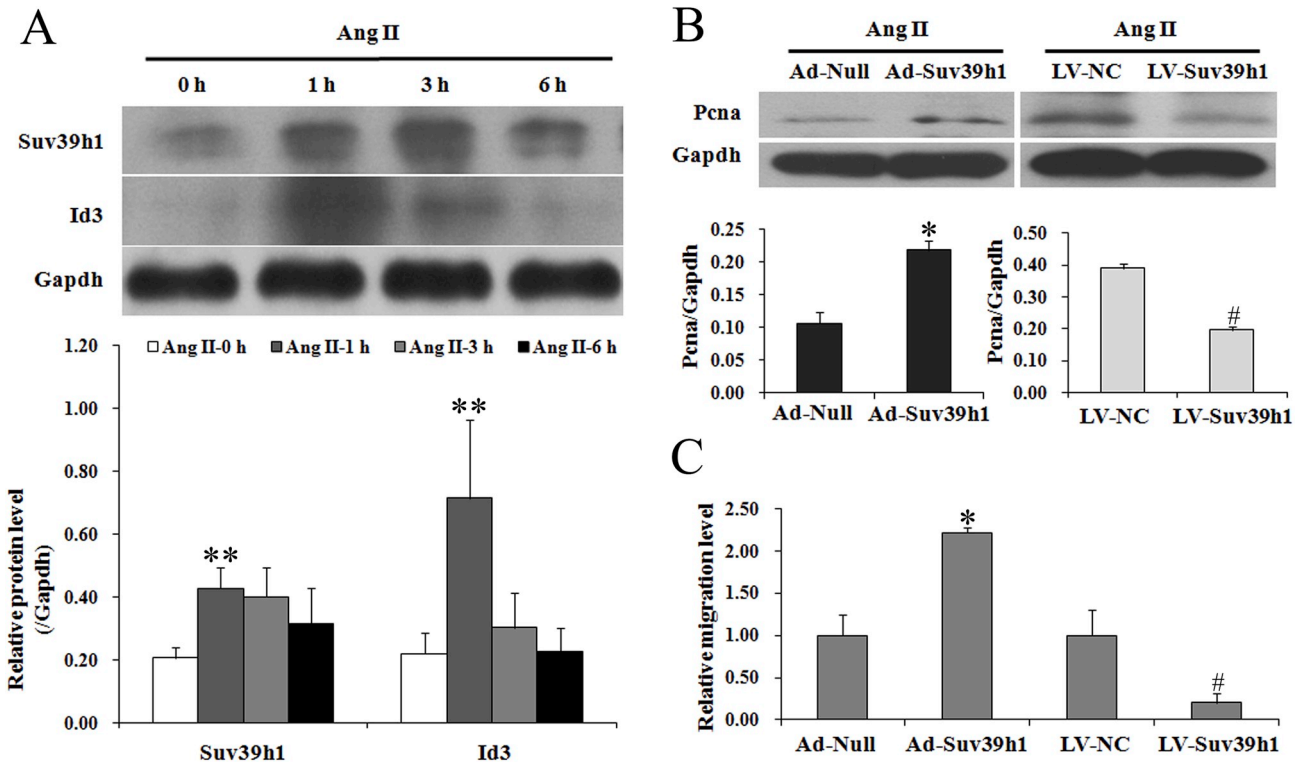

Fig. 1. Suv39h1 plays a crucial role in Ang II-induced VSMCs proliferation and migration.
(A) The change in Suv39h1 and Id3 protein expression stimulated by Ang II for different durations was examined by Western blotting. (B) The proliferation of VSMCs was evaluated by examining protein expression of Pcna. Representative gel images are shown in the upper panel and quantification (the ratio relative to the internal control protein Gapdh) in the lower panel. (C) The migration of VSMCs was examined using the Transwell method. It is represented as fold change relative to the corresponding control group. $^{**}p < 0.05$, compared with the 0 h group (n = 3). $^{*}p < 0.05$, compared with the Ad-Null group; $^{\#}p < 0.05$, compared with the LV-NC group (n = 3). The results are representative of three independent experiments.

2.9. Statistical analysis

All statistical analysis was conducted using SPSS 17.0 software. Quantitative data are presented as means ± SD. Student's *t*-test was used for comparisons between two groups and one-way ANOVA was used for multiple comparisons. Tukey's honestly significant difference test was used for pairwise comparisons among multiple samples. $p < 0.05$ was considered statistically significant.

3. Results

3.1. The inhibitory effect of LV-Suv39h1 on Suv39h1 mRNA expression

Four different LV-Suv39h1 shRNA were transfected into VSMCs with MOI = 40 for 96 h. Compared with the NC group, the knockdown efficiency of *Suv39h1* in the KD2 group was 52%, in the KD3 and KD4 groups it was over 60%, and in the KD1 group it was over 80% (Supplementary Fig. 1). As KD1 had the best silencing effect on *Suv39h1*, it was selected for subsequent experiments.

3.2. Ang II transiently stimulates Suv39h1 and Id3 expression in VSMCs

In VSMCs stimulated with 0.2 μg/ml Ang II for 1 h, Suv39h1 expression approximately doubled that in the control (CON) group (Fig. 1A). However, at 6 h after Ang II stimulation, the Suv39h1 expression was lower than that at 1 and 3 h, and was not significantly different from that in the CON group. Furthermore, at 1 h after Ang II stimulation, Id3 expression was 1.2-fold increase than that in the CON group. However, after longer stimulation (3 and 6 h), Id3 expression gradually decreased, approaching pre-stimulation levels at 6 h (Fig. 1A).

3.3. Suv39h1 downregulation inhibits migration and proliferation of Ang II-stimulated VSMCs

Transected with Ad-Suv39h1, proliferation and migration of Ang II-stimulated VSMCs significantly increased. Compared with the Ad-Null group, Pcna protein expression (Fig. 1B), an indicator of cell proliferation [15], and the number of migrating cells (Fig. 1C) in the Ad-Suv39h1 group were significantly increased. In contrast, after Suv39h1 knockdown, migration and proliferation of Ang II-stimulated VSMCs were significantly inhibited. Compared with the LV-NC group, Pcna expression in the LV-Suv39h1 group decreased to 50% and the number of migrating cells was 80% lower (Fig. 1B and C, respectively).

3.4. Suv39h1 participates in the regulation of Ang II-induced Id3 expression and the activation of its downstream genes via modulation of H3K9me3 at the proximal promoter region

After Suv39h1 expression was upregulated in VSMCs by Ad-Suv39h1 transfection, cells were stimulated for 1 h with Ang II. Id3 expression was 1.6-fold increase in cells transfected with Ad-Suv39h1 compared with the control, and p21 and p27Kip1 protein levels were decreased by 52% and 40%, respectively (Fig. 2A). Conversely, after transfection of cells with LV-*Suv39h1*, Id3 expression decreased by 50%, compared with the LV-NC group, which was consistent with the decrease in Suv39h1 expression. In contrast, the p21 and p27Kip1 levels increased by 75% and 62%, respectively, in the LV-Suv39h1 group (Fig. 2A).

H3K9me3 is the main substrate of Suv39h1, which correlates with gene repression. To determine whether the upregulation of *p21* and *p27Kip1* is due to the inhibition of H3K9me3 after Suv39h1 downregulation, western blotting was performed to examine the total

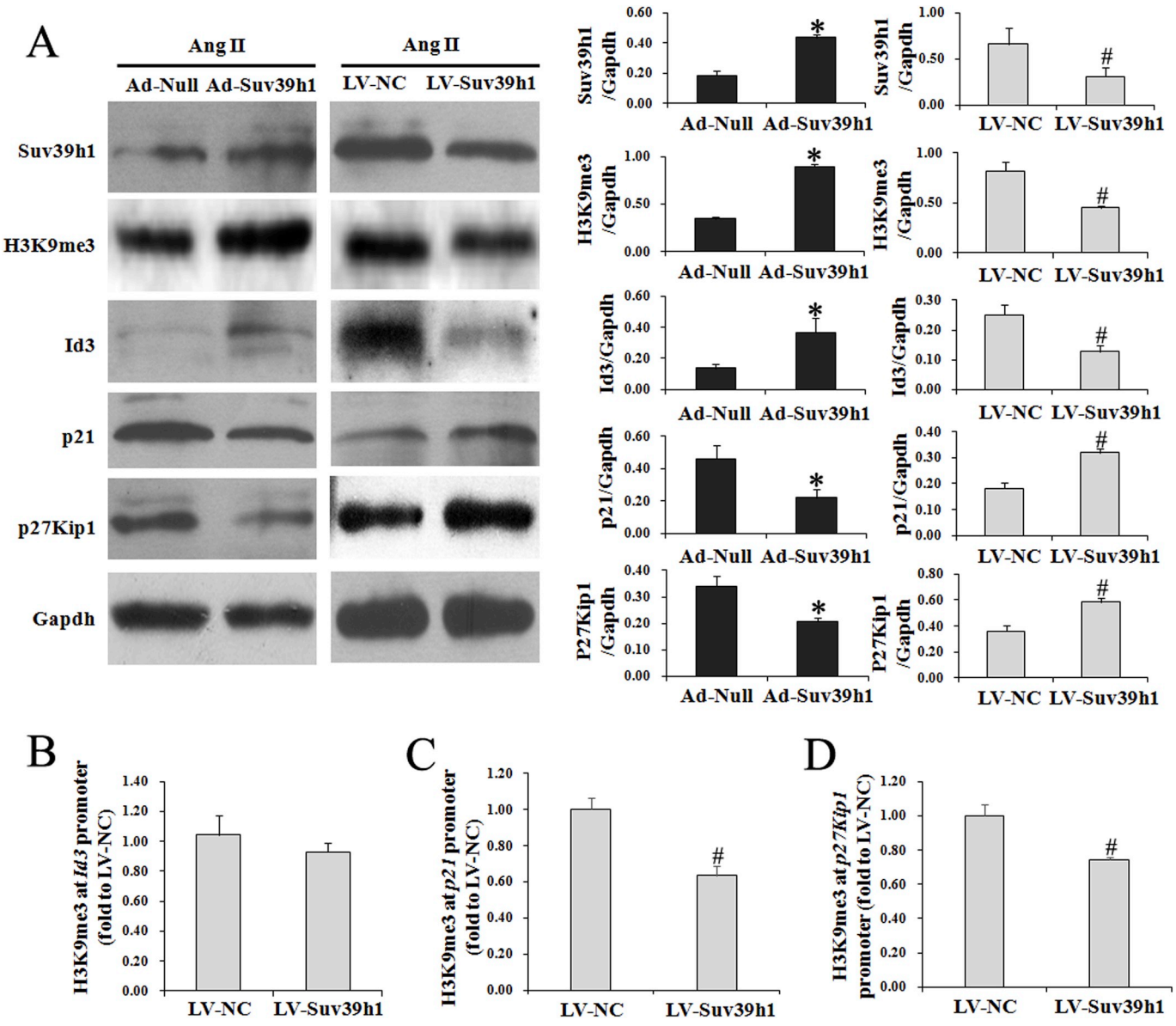

Fig. 2. Suv39h1 is the key regulator of Id3, p21 and p27Kip1 induced by Ang II.
(A) Protein expression changes in Suv39h1, H3K9me3, Id3, p21 and p27Kip1 after transfection with Ad-Suv39h1, Ad-Null, LV- Suv39h1 or LV-NC. (B-D) H3K9me3 levels at the promoters of *Id3* (B), *p21* (C) and *p27Kip1* (D) in VSMCs were quantified by ChIP-PCR. The protein expression is relative to Gapdh. $^{*}p < 0.05$, compared with Ad-Null group; $^{\#}p < 0.05$, compared with LV-NC group (n = 3). The results are representative of three independent experiments.

H3K9me3 level. As shown in Fig. 2A, H3K9me3 increased after Suv39h1 upregulation in Ang II-treated VSMCs, whereas Suv39h1 knockdown displayed an inhibiting effect. Furthermore, ChIP-qPCR assays indicated that although there was no significant difference in H3K9me3 expression in the proximal promoter region of *Id3* (Fig. 2B, $p > 0.05$), H3K9me3 at the promoters of *p21* and *p27Kip1* was decreased by nearly 40% and 30%, respectively, due to Suv39h1 knockdown in VSMCs under Ang II stimulation (Fig. 2C and D). These results suggest that Suv39h1 regulated *p21* and *p27Kip1* transcription by controlling H3K9me3 at their proximal promoter region.

3.5. Balloon injury induces Suv39h1 and Id3 expression

In blood vessels with balloon injury, *Suv39h1* and *Id3* expression was upregulated. Compared with the sham operation group, the *Suv39h1* mRNA levels in the model group were nearly 1.2-fold increase (Fig. 3A) and the *Id3* mRNA levels increased by 90% (Fig. 3B) at 7 days after injury ($p < 0.05$).

3.6. Suv39h1 regulates Id3 and H3K9me3 activation after vascular injury

The efficiency of local virus infection was optimal 7 days after injury (Supplementary Fig. 2). The H3K9me3 level was enhanced in the Ad-Suv39h1 group, but suppressed by Suv39h1 knockdown in blood vessels at 28 d after balloon injury (Fig. 3C). Ad-Suv39h1 was transfected into blood vessels of rats after balloon injury, resulting in a nearly 7-fold upregulation of *Suv39h1* mRNA expression. Concomitantly, the *Id3* mRNA expression increased by 97% in the Ad-Suv39h1 group than in the Ad-Null group. After LV-*Suv39h1* was transfected into injured blood vessels, the *Suv39h1* levels decreased by nearly 42% and those of *Id3* by 31%, compared with the LV-NC group (Fig. 3D–G). Along with the *Id3* change, the expression of *p21* and *p27 Kip1* was suppressed by Suv39h1 upregulation (Fig. 3H and J) and increased by Suv39h1 downregulation (Fig. 3I and K).

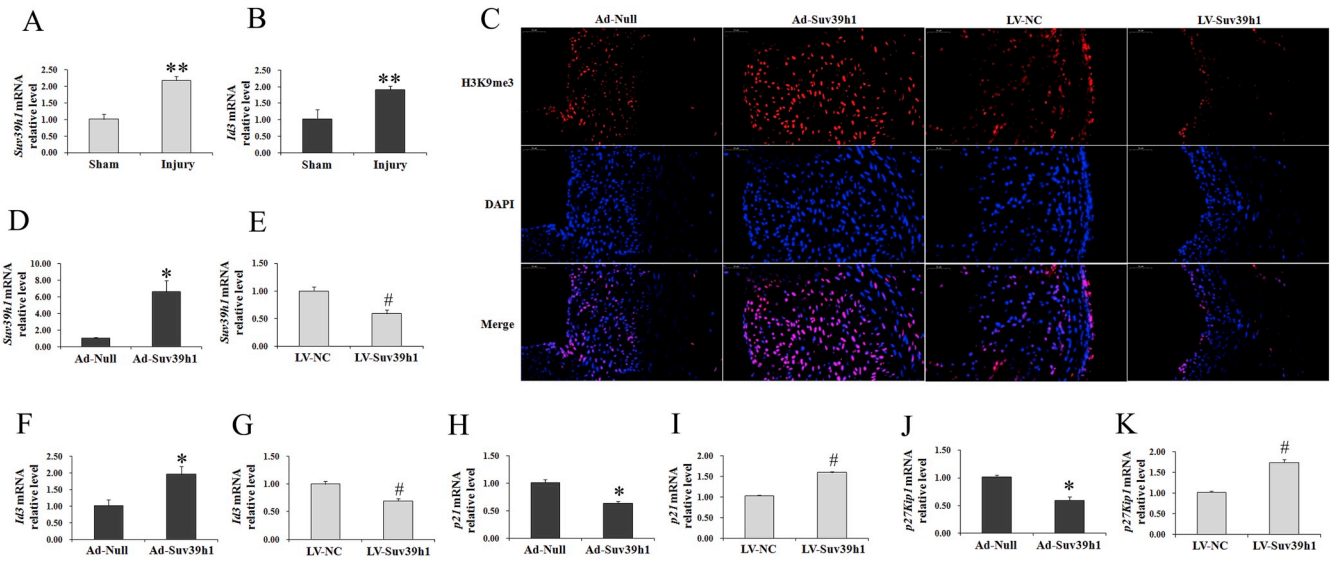

Fig. 3. Suv39h1 plays a vital regulation role in the expression of *Id3* and total H3K9me3 under vascular injury.
Real-time PCR was used to examine the mRNA expression of *Suv39h1* and *Id3* on day 7 after balloon injury. The mRNA expression of *Suv39h1* (A) and *Id3* (B) is displayed as fold change compared with the sham operation group. The total H3K9me3 levels in carotid arteries on day 28 after balloon injury were determined by immunofluorescence staining (C). The mRNA expression of *Suv39h1*, *Id3*, *p21* and *p27Kip1* after transfection with Ad-Suv39h1, Ad-Null (D, F, H and J), LV-Suv39h1 or LV-NC (E, G, I and K) was examined by real-time PCR. *Gapdh* was used for normalization. Red denotes the immunofluorescence of H3K9me3. Blue denotes nuclear staining by DAPI. $^{**}p < 0.05$, compared with the sham group. $^{*}p < 0.05$, compared with the Ad-Null group; $^{\#}p < 0.05$, compared with the LV-NC group. The results are representative of three separate experiments. Three carotid arteries were pooled in each experiment. (For interpretation of the references to colour in this figure legend, the reader is referred to the Web version of this article.)

3.7. Suv39h1 downregulation inhibits neointimal hyperplasia after vascular injury

Vascular histological staining on day 28 after balloon injury indicated that Suv39h1 overexpression promoted intimal hyperplasia. Compared with the Ad-Null group, the neointimal area in the Ad-Suv39h1 group was increased by 75% ($p = 0.049$) and the intima/media ratio was increased by 84%. After Suv39h1 downregulation, neointima formation was significantly inhibited. Compared with the LV-NC group, the intimal area in the LV-Suv39h1 group was reduced by nearly 72% and the intima/media ratio was decreased by 64% (Fig. 4A).

3.8. Suv39h1 downregulation inhibits neointimal Pcna expression

Suv39h1 overexpression promoted Pcna expression in the neointima, while Suv39h1 downregulation inhibited this injury-induced change. The ratio of Pcna-positive cells in the Ad-Suv39h1 group was 35% higher than that in the Ad-Null group. In the LV-Suv39h1 group, it was 30% lower than that in the LV-NC group (Fig. 4B).

3.9. Suv39h1 downregulation inhibits collagen deposition after vascular injury

Collagen, the main component of extracellular matrix (ECM) secreted by proliferating VSMCs, was expressed at a higher level in arteries transfected with Ad-Suv39h1, but at a lower level in arteries transfected with LV-Suv39h1, compared with the corresponding control groups. The collagen area ratio in the Ad-Suv39h1 group was 2.02-fold than that in the Ad-Null group. In the LV-Suv39h1 group, it was reduced by 44% compared with the LV-NC group (Fig. 4C).

4. Discussion

The results of this study suggest that Suv39h1 plays an important regulatory role during pathological activation of VSMCs that causes neointimal hyperplasia after vascular injury. Suv39h1 overexpression promoted migration and proliferation of VSMCs stimulated by Ang II *in vitro*, and neointima formation after balloon injury *in vivo*. Furthermore, Suv39h1 downregulation significantly inhibited pathological activation of VSMCs, and attenuated pathological remodeling after vascular injury. The Suv39h1 mechanism of action may be through affecting the expression of the downstream proteins p21 and p27Kip1 via Id3 regulation and H3K9me3 modulation.

Consistent with previous studies [16], our results demonstrated that Ang II stimulation induced increased Id3 expression in VSMCs. Unlike the earlier studies, our time course experiments showed that the expression of both Suv39h1 and Id3 reached peak values at 1 h after Ang II stimulation, and then gradually decreased to pre-stimulation levels. The consistent time-dependent changes in Suv39h1 and Id3 expression suggests that Id3 is a regulatory factor in the biological effects of Suv39h1 in VSMCs. This hypothesis was further supported by our findings that Id3 was upregulated and downregulated by Suv39h1 overexpression and shRNA silencing, respectively. However, suppression of Id3 by Suv39h1 silencing is not necessarily associated with the increase in H3K9me3 at the target promoters, as demonstrated by previous results [17]. One possibility is that other repressive histone markers have been deposited to cause the repression. H3K4me3 and H3K27me3 can also bind to the *Id3* promoter [18], thus Suv39h1 downregulation would suppress H3K4me3, resulting in Id3 knockdown. In addition, neither H3K27me3 nor H3K9me3 changed at the *HER2* promoter when Suv39h1 was overexpressed by the dCas9 method [17], which indicated the transcription regulation by Suv39h1 may not completely require histone methylation.

Similar to E12 and E47 from the common E2A family, Id3 can bind to transcription factors such as MyoD, Pax and TCF, and inhibit DNA binding, and thus transcription [7,19–21]. It has recently been shown that the KIP/CIP subclasses of the CDKIs, including p21 and p27Kip1, also affected protein binding by Id3 [10,11]. As broad spectrum CDKIs, p21 and p27Kip1 can bind to almost all CDKs to inhibit key integration factors of the mitotic pathway, leading to cell cycle arrest [22]. Under Ang II stimulation, the induced Id3 can bind to p21 and p27Kip1, promoting increased levels of free CDKs. This induces VSMCs to enter an active division and proliferation stage. In contrast, Suv39h1

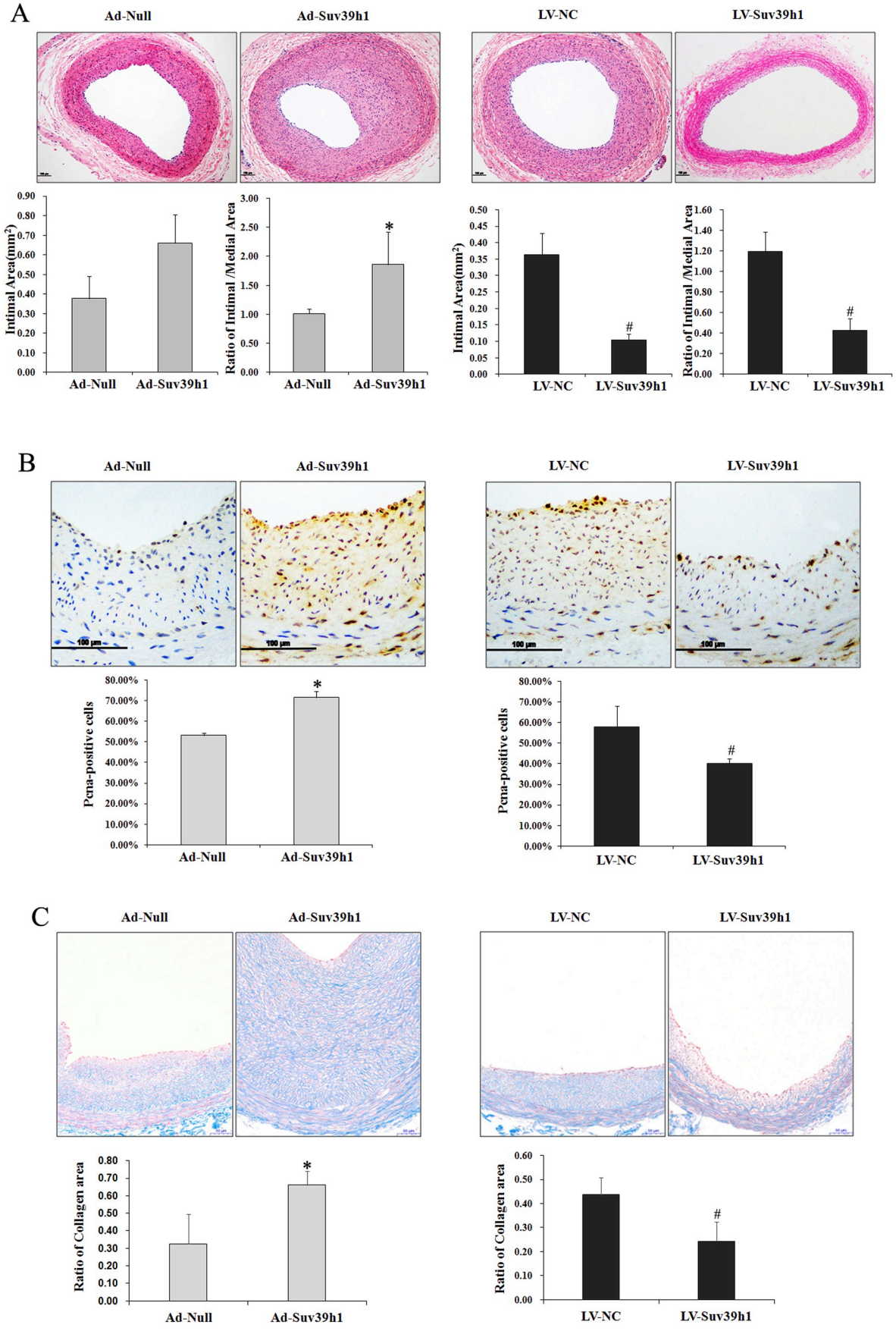

(caption on next page)

Fig. 4. Suv39h1 significantly inhibits neointimal hyperplasia under balloon injury.
H&E staining was performed for each group to measure the medial area (MA), intimal area (IA) and I/M ratio 28 days after balloon injury (A). Immunohistochemistry analysis of Pcna expression in neointima was performed on day 28 after balloon injury (B). Pcna labeled nuclei are dark brown. The left side is a representative image of each group; the right side is the Pcna-positive cell ratio. Representative Masson's trichrome-stained photomicrographs of carotid arteries from different groups were also taken on day 28 after balloon injury (C). Collagen is blue. $^{*}p < 0.05$, compared with the Ad-Null group; $^{\#}p < 0.05$, compared with the LV-NC group. The results are representative of six separate experiments. (For interpretation of the references to colour in this figure legend, the reader is referred to the Web version of this article.)

downregulation decreases Id3 binding to p21 and p27Kip1, leading to increased p21 and p27Kip1 levels and DNA binding. This promotes inhibition of VSMC proliferation. Consistent with a previous study [23], Suv39h1 downregulation also promoted p21 and p27Kip1 expression by inhibiting methylation of promoter regions, leading to inhibition of VSMCs proliferation under pathological stimulation. Previous studies have confirmed that p27Kip1 overexpression significantly inhibited *Suv39h1* transcription [24]. Therefore, we hypothesized that Suv39h1, Id3 and p27Kip1 form a regulatory feedback loop. Suv39h1 downregulation induces p21 and p27Kip1 expression through two pathways. First, Id3 downregulation decreases its binding to p21 and p27Kip1. Second, decreased histone H3K9 trimethylation at the *p21* and *p27Kip1* promoter regions after Suv39h1 downregulation increases p21 and p27Kip1 expression. In addition, increased expression of p27Kip1 further inhibits *Suv39h1* transcription, enhancing the inhibition of cell cycle activation associated with Suv39h1 downregulation.

As a member of the histone methyltransferase family, Suv39h1 has a conserved SET catalytic domain, inhibiting transcription through H3K9 methylation [25], and it plays a vital role in diabetes-induced “metabolic memory” and “inflammatory memory” [26]. By inhibiting Suv39h1 and H3K9 methylation, miR-125b promotes IL-6 and MCP-1 expression in VSMCs, inducing diabetes and aggravating the inflammatory response [27]. However, it is unclear whether miR-125b inhibits proliferation and migration of VSMCs. Suv39h1 overexpression promoted trimethylation of H3K9 at the *NF-κB*, *IL-6*, *MCP-1* and *caspase 3* promoter regions when renal tubular epithelial cells were stimulated by high glucose. This resulted in significant anti-inflammatory and antioxidant effects, thereby inhibiting apoptosis [28]. Recently, oncology studies have shown that Suv39h1 inhibited the transduction of apoptosis-related signals by promoting trimethylation of the apoptosis-inducing genes, *Fas* and *PUMA*, thereby promoting the occurrence of glioblastoma [29]. In addition, Suv39h1 induced breast cancer cell proliferation through modified methylation of the tumor suppressor gene, *RASSF8* [30]. The level of H3K9 trimethylation in the erosive tissue of colon cancer was significantly higher than in normal tissue, and Suv39h1 overexpression increased tumorigenicity and mortality in mice [31]. Furthermore, metformin inhibited migration of prostate cancer cells through Suv39h1 downregulation [32]. Another study has demonstrated that vascular injury was accompanied by an imbalance in expression of proliferative and anti-proliferative factors [33]. However, a few studies have revealed that Suv39h1 suppressed cell proliferation via H3K9me3 at the promoters of oncogenes. Methylation of *Sp1* increased the recruitment of Suv39h1 to the *cyclin B1* promoter, which resulted in trimethylation of H3K9 and subsequent downregulation of cyclin B1, leading to cell cycle arrest at the G2 phase [34]. Global gene expression analysis revealed that cyclins, polo-like kinase and other cell cycle regulators were significantly decreased in Suv39h1-overexpressing fish, which indicated that Suv39h1 may be a suppressor of rhabdomyosarcoma formation [35]. This study found that Suv39h1, a transcriptional inhibitor, has a weaker effect on the proliferation-related gene, Id3, than the anti-proliferative-related genes, *p21* and *p27Kip1*, thus resulting in pathological activation of VSMCs and neointima formation. This evidence suggests that the effect and mechanism of Suv39h1 on cell proliferation is complicated and depends on cell type, stimulus and intervention strategy. However, further research is required to fully elucidate the mechanism.

In conclusion, downregulation of Suv39h1 can effectively inhibit neointima formation after vascular injury, which provides a new intervention target for the prevention and treatment of proliferative vascular diseases like restenosis.

Conflicts of interest

The authors declared they do not have anything to disclose regarding conflict of interest with respect to this manuscript.

Financial support

This work was supported by the National Natural Science Foundation of China (81500230, 81470387, 81770360, 81670333, 81770456, 81600234), Hubei Province Health and Family Planning Scientific Research Project (WJ2019Z004), and Hubei Provincial Natural Science Foundation (2018CFA044).

Author contributions

Jing Zhang conceived the study, and wrote and reviewed the manuscript. Jing Chen and Qi Hu performed molecular experiments. Wenqi Gao and Hui Wu performed histological and statistical analysis. Changwu Xu and Chaojun Yang performed animal surgery and collected vessel samples. Qing Guo and Wanyin Cai performed cell culture and sample collection. Jun Yang and Chao He reviewed the manuscript. Jian Yang conceived the study and reviewed the manuscript.

Appendix A. Supplementary data

Supplementary data to this article can be found online at https://doi.org/10.1016/j.atherosclerosis.2019.06.909.

References

[1] S. Cassese, R.A. Byrne, T. Tada, S. Pinieck, M. Joner, T. Ibrahim, L.A. King, M. Fusaro, K.L. Laugwitz, A. Kastrati, Incidence and predictors of restenosis after coronary stenting in 10 004 patients with surveillance angiography, Heart 100 (2014) 153–159.
[2] S.O. Marx, H. Totary-Jain, A.R. Marks, Vascular smooth muscle cell proliferation in restenosis, Circ. Cardiovasc. Interv. 4 (2011) 104–111.
[3] D. Wang, P. Uhrin, A. Mocan, B. Waltenberger, J.M. Breuss, D. Tewari, J. Mihaly-Bison, L. Huminiecki, R.R. Starzynski, N.T. Tzvetkov, J. Horbanczuk, A.G. Atanasov, Vascular smooth muscle cell proliferation as a therapeutic target. Part 1: molecular targets and pathways, Biotechnol. Adv. 36 (2018) 1586–1607.
[4] C.J. Sherr, J.M. Roberts, CDK inhibitors: positive and negative regulators of G1-phase progression, Genes Dev. 13 (1999) 1501–1512.
[5] S.R. Datla, L. L Hilenski, B. Seidel-Rogol, A.E. Dikalova, M. Harousseau, L. Punkova, G. Joseph, W.R. Taylor, B. Lassegue, K.K. Griendling, Poldip2 knockdown inhibits vascular smooth muscle proliferation and neointima formation by regulating the expression of PCNA and p21, Lab. Invest. 99 (2019) 387–398.
[6] Y. Xu, Y. Bei, S. Shen, J. Zhang, Y. Lu, J. Xiao, X. Li, MicroRNA-222 promotes the proliferation of pulmonary arterial smooth muscle cells by targeting P27 and TIMP3, cell, Physiol. Biochem. 43 (2017) 282–292.
[7] E.C. Roberts, R.W. Deed, T. Inoue, J.D. Norton, A.D. Sharrocks, Id helix-loop-helix proteins antagonize pax transcription factor activity by inhibiting DNA binding, Mol. Cell. Biol. 21 (2001) 524–533.
[8] M.E. Matsumura, F. Li, L. Berthoux, B. Wei, D.R. Lobe, C. Jeon, M.L. Hammarskjold, C.A. McNamara, Vascular injury induces posttranscriptional regulation of the Id3 gene: cloning of a novel Id3 isoform expressed during vascular lesion formation in rat and human atherosclerosis, Arterioscler. Thromb. Vasc. Biol. 21 (2001) 752–758.
[9] H. Deliri, N. Meller, A. Kadakkal, R. Malhotra, J. Brewster, A.C. Doran, H. Pei, S.N. Oldham, M.D. Skaflen, J.C. Garmey, C.A. McNamara, Increased 12/15-lipoxygenase enhances cell growth, fibronectin deposition, and neointimal formation in response to carotid injury, Arterioscler. Thromb. Vasc. Biol. 31 (2011) 110–116.

[10] C.A. O'Brien, A. Kreso, P. Ryan, K.G. Hermans, L. Gibson, Y. Wang, A. Tsatsanis, S. Gallinger, J.E. Dick, ID1 and ID3 regulate the self-renewal capacity of human colon cancer-initiating cells through p21, Cancer Cell, 21 (2012) 777–792.
[11] A. Chassot, L. Turchi, T. Virolle, G. Fitsialos, M. Batoz, M. Deckert, V. Dulic, G. Meneguzzi, R. Busca, G. Ponzio, Id3 is a novel regulator of p27kip1 mRNA in early G1 phase and is required for cell-cycle progression, Oncogene 26 (2007) 5772–5783.
[12] L. Cai, X. Ma, Y. Huang, Y. Zou, X. Chen, Aberrant histone methylation and the effect of Suv39H1 siRNA on gastric carcinoma, Oncol. Rep. 31 (2014) 2593–2600.
[13] T. Cherrier, S. Suzanne, L. Redel, M. Calao, C. Marban, B. Samah, R. Mukerjee, C. Schwartz, G. Gras, B.E. Sawaya, S.L. Zeichner, D. Aunis, C. Van Lint, O. Rohr, p21(WAF1) gene promoter is epigenetically silenced by CTIP2 and SUV39H1, Oncogene 28 (2009) 3380–3389.
[14] J. Chen, J. Zhang, J. Yang, L. Xu, Q. Hu, C. Xu, S. Yang, H. Jiang, Histone demethylase KDM3a, a novel regulator of vascular smooth muscle cells, controls vascular neointimal hyperplasia in diabetic rats, Atherosclerosis 257 (2017) 152–163.
[15] D. Gordon, M.A. Reidy, E.P. Benditt, S.M. Schwartz, Cell proliferation in human coronary arteries, Proc. Natl. Acad. Sci. U. S. A 87 (1990) 4600–4604.
[16] C. Mueller, S. Baudler, H. Welzel, M. Bohm, G. Nickenig, Identification of a novel redox-sensitive gene, Id3, which mediates angiotensin II-induced cell growth, Circulation 105 (2002) 2423–2428.
[17] H. O'Geen, C. Ren, C.M. Nicolet, A.A. Perez, J. Halmai, V.M. Le, J.P. Mackay, P.J. Farnham, D.J. Segal, dCas9-based epigenome editing suggests acquisition of histone methylation is not sufficient for target gene repression, Nucleic Acids Res. 45 (2017) 9901–9916.
[18] S. He, Y. Liu, L. Meng, H. Sun, Y. Wang, Y. Ji, J. Purushe, P. Chen, C. Li, J. Madzo, J. Issa, J. Soboloff, R. Reshef, B. Moore, L. Gattinoni, Y. Zhang, Ezh2 phosphorylation state determines its capacity to maintain CD8(+) T memory precursors for antitumor immunity, Nat. Commun. 8 (2017) 2125.
[19] M.E. Massari, C. Murre, Helix-loop-helix proteins: regulators of transcription in eucaryotic organisms, Mol. Cell. Biol. 20 (2000) 429–440.
[20] D.A. Loveys, M.B. Streiff, G.J. Kato, E2A basic-helix-loop-helix transcription factors are negatively regulated by serum growth factors and by the Id3 protein, Nucleic Acids Res. 24 (1996) 2813–2820.
[21] P.R. Yates, G.T. Atherton, R.W. Deed, J.D. Norton, A.D. Sharrocks, Id helix-loop-helix proteins inhibit nucleoprotein complex formation by the TCF ETS-domain transcription factors, EMBO J. 18 (1999) 968–976.
[22] C.J. Sherr, J.M. Roberts, CDK inhibitors: positive and negative regulators of G1-phase progression, Genes Dev. 13 (1999) 1501–1512.
[23] S.H. Lin, W.T. Ho, Y.T. Wang, C.T. Chuang, L.Y. Chuang, J.Y. Guh, Histone methyltransferase Suv39h1 attenuates high glucose-induced fibronectin and p21(WAF1) in mesangial cells, Int. J. Biochem. Cell Biol. 78 (2016) 96–105.
[24] G. Yildirim-Buharalioglu, M. Bond, G.B. Sala-Newby, C.C. Hindmarch, A.C. Newby, Regulation of epigenetic modifiers, including KDM6B, by interferon-gamma and interleukin-4 in human macrophages, Front. Immunol. 8 (2017) 92.
[25] M. Lachner, T. Jenuwein, The many faces of histone lysine methylation, Curr. Opin. Cell Biol. 14 (2002) 286–298.
[26] L.M. Villeneuve, M.A. Reddy, L.L. Lanting, M. Wang, L. Meng, R. Natarajan, Epigenetic histone H3 lysine 9 methylation in metabolic memory and inflammatory phenotype of vascular smooth muscle cells in diabetes, Proc. Natl. Acad. Sci. U. S. A 105 (2008) 9047–9052.
[27] L.M. Villeneuve, M. Kato, M.A. Reddy, M. Wang, L. Lanting, R. Natarajan, Enhanced levels of microRNA-125b in vascular smooth muscle cells of diabetic db/db mice lead to increased inflammatory gene expression by targeting the histone methyltransferase Suv39h1, Diabetes 59 (2010) 2904–2915.
[28] J. Wang, W. Yan, X. Peng, Y. Jiang, L. He, Y. Peng, X. Chen, M. Ye, H. Zhuo, Functional role of SUV39H1 in human renal tubular epithelial cells under high-glucose ambiance, Inflammation 41 (2018) 1–10.
[29] X. Lai, Z. Deng, H. Guo, X. Zhu, W. Tu, HP1alpha is highly expressed in glioma cells and facilitates cell proliferation and survival, Cancer Biomark. 20 (2017) 453–460.
[30] I.P. Karthik, P. Desai, S. Sukumar, A. Dimitrijevic, K. Rajalingam, S. Mahalingam, E4BP4/NFIL3 modulates the epigenetically repressed RAS effector RASSF8 function through histone methyltransferases, J. Biol. Chem. 293 (2018) 5624–5635.
[31] Y. Yokoyama, M. Hieda, Y. Nishioka, A. Matsumoto, S. Higashi, H. Kimura, H. Yamamoto, M. Mori, S. Matsuura, N. Matsuura, Cancer-associated upregulation of histone H3 lysine 9 trimethylation promotes cell motility in vitro and drives tumor formation in vivo, Cancer Sci. 104 (2013) 889–895.
[32] T. Yu, C. Wang, J. Yang, Y. Guo, Y. Wu, X. Li, Metformin inhibits SUV39H1-mediated migration of prostate cancer cells, Oncogenesis 6 (2017) e324.
[33] S.M. Seedial, S. Ghosh, R.S. Saunders, P.A. Suwanabol, X. Shi, B. Liu, K.C. Kent, Local drug delivery to prevent restenosis, J. Vasc. Surg. 57 (2013) 1403–1414.
[34] J. Chuang, W. Chang, J. Hung, Hydrogen peroxide induces Sp1 methylation and thereby suppresses cyclin B1 via recruitment of Suv39H1 and HDAC1 in cancer cells, Free Radic. Biol. Med. 51 (2011) 2309–2318.
[35] C.E. Albacker, N.Y. Storer, E.M. Langdon, A. Dibiase, Y. Zhou, D.M. Langenau, L.I. Zon, The histone methyltransferase SUV39H1 suppresses embryonal rhabdomyosarcoma formation in zebrafish, PLoS One 8 (2013) e64969.